NIPPON STEEL TECHNICAL REPORT No. 92 July 2005

UDC 624 . 155 . 8

Study on Uplift Resistance of Screwed Steel Pile

Makoto NAGATA*1 Hisashi HIRATA*2

Abstract

A screwed steel pipe pile exerts a huge resistance at the lower end against an uplifting load owing to the anchoring effect of the spiral wing provided at the pile end. Uplift tests of reduced-scale screwed pipe piles using purpose-made model test equipment clarified the relationship between pile diameter, wing diameter, pile-end depth and the uplift resistance at the pile end. Visible tests and earth pressure measurement with reduced-scale piles carried out after the above disclosed the soil movement and earth pressure near the pile end at pile driving and uplifting. Based on these results, the shape of the shear fracture zone of soil that brought about the uplift resistance was estimated.

1. Introduction

A screwed pile is a steel pipe pile with a spiral wing provided at the lower end (toe) to drill into soil (see **Fig. 1**). Since the pile is driven into soil under rotating torque, it is not necessary to remove soil for pile driving. Tensile loading tests of real-size screwed piles have disclosed that this type of pile has a large pile-end uplift resistance owing to the anchoring effect of the wing spirally driven into soil[1,2]. However, there have been only a limited number of studies on the uplift resistance of a screwed pile, and many aspects of the resistance remain unclear.

The present paper reports uplifting tests of reduced-scale screwed piles using purpose-made test facilities for reduced-scale specimens[3] and the analysis of the characteristics of the pile-end uplift resistance based on the results of the tests. The paper also reports the investigation of the soil region in which shear fracture occurs by actual observation of sand movement, the measurement of earth pressure during driving and uplifting of piles, and studies on the magnitude and distribution of earth pressure acting on the shear fracture zone of soil based on the results of the above tests and measurement.

2. Uplifting Test

2.1 Outline of test equipment

The authors drove model piles to prescribed depths by rotation and then conducted loading tests (or uplifting tests) in the same manner as explained in reference[3] using the following facilities and specimens: (A) a cylindrical sand-soil tank 1,200 mm in height and 1,200 mm in diameter filled with silica sand No. 6 having a relative density of 84% and equipped with pressurizing facilities; (B) a pile-driving and loading device for applying torque and vertical uplifting load to specimen piles at the top; (C) reduced-scale double-tube model piles; and (D) a measurement device for real-time monitoring of the torque and axial force.

2.2 Test parameters

In order to study the relationship between uplift resistance and the depth of a pile end, the pile-end depth was changed from 100 to 800 mm. In addition, for studying the influence of the wing diameter ratio (Rd), specimen piles 40 mm in pile diameter (Dp) having wing diameters 1.5 to 3.0 times the pile diameter were prepared. Further, for studying the influence of the wing diameter ratio, speci-

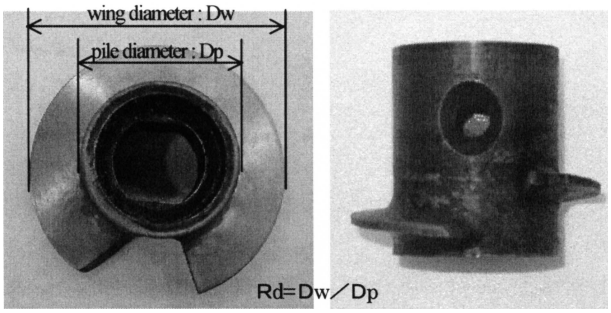

Fig. 1 Pile toe

*1 Building Construction Division

*2 Steel Research Laboratories

Table 1 Test parameter

Test case No.	Test name	Dp (mm)	Rd	Dw (mm)	Pile toe depth (mm)	Confining pressure		Pile top load (kN)
						Axial (kPa)	Lateral (kPa)	
1	4D15W3P10L3S10H	40	1.5	60	100	300	150	1
2	4D15W3P10L3S30H	40	1.5	60	300	300	150	1
3	4D15W3P10L3S60H	40	1.5	60	600	300	150	1
4	4D15W3P10L3S80H	40	1.5	60	800	300	150	1
5	4D175W3P10L3S10H	40	1.75	70	100	300	150	1
6	4D175W3P10L3S30H	40	1.75	70	300	300	150	1
7	4D175W3P10L3S60H	40	1.75	70	600	300	150	1
8	4D175W3P10L3S80H	40	1.75	70	800	300	150	1
9	4D20W3P10L3S10H	40	2.0	80	100	300	150	1
10	4D20W3P10L3S30H	40	2.0	80	300	300	150	1
11	4D20W3P10L3S60H	40	2.0	80	600	300	150	1
12	4D20W3P10L3S80H	40	2.0	80	800	300	150	1
13	4D25W3P10L3S10H	40	2.5	100	100	300	150	1
14	4D25W3P10L3S30H	40	2.5	100	300	300	150	1
15	4D25W3P10L3S60H	40	2.5	100	600	300	150	1
16	4D25W3P10L3S80H	40	2.5	100	800	300	150	1
17	4D30W3P10L3S10H	40	3.0	120	100	300	150	1
18	4D30W3P10L3S30H	40	3.0	120	300	300	150	1
19	4D30W3P10L3S60H	40	3.0	120	600	300	150	1
20	4D30W3P10L3S80H	40	3.0	120	800	300	150	1
21	5D20W3P10L3S60H	50	2.0	100	600	300	150	1
22	6D167W3P10L3S60H	60	1.67	100	600	300	150	1

men piles 100 mm in wing diameter (Dw) having pile diameters of 40, 50 and 60 mm were also prepared. **Table 1** shows the combinations of the test parameters. The confining pressures of the soil were set as follows for all the specimens: the axial pressure at 300 kPa and the lateral pressure at 150 kPa. The load imposed on the top of a pile during pile driving (pile top axial force) was set at 1 kN also for all the specimens.

3. Test Results

3.1 General

Fig. 2 shows a typical example of the test results. What is shown is the result of Case 11, where the pile diameter was 40 mm, the wing diameter was 80 mm, and the pile end depth was 600 mm. Here, the axial force at the pile top is that applied to the pile top, the resistance at the pile end is the axial force measured just below the end of a double-tube specimen pile, and the friction on the pile surface is that measured at the top of the same. The displacement of a pile was measured at the pile top.

One sees here that the pile-end uplift resistance hit a maximum at a displacement of roughly 14 mm (0.35 Dp), and then decreased to a residual resistance of roughly 65% of the maximum as the pile was lifted further. The surface friction hit a maximum at a displacement of roughly 6 mm, and then decreased to a residual resistance of roughly 75% of the maximum. These tendencies were substantially the same with all the specimens.

3.2 Analysis of uplift resistance

Fig. 3 shows the relationship between pile-end depth and uplift resistance. With all the wing diameters, the pile-end uplift resistance tended to converge upon a certain value when the depth was larger than a certain value. This seems to indicate that the fracture zone of the sand soil resulting from the anchoring effect of the pile-end wing does not expand more than a certain extent.

Next, **Fig. 4** shows the relationship between wing diameter ratio (Rd) and pile-end uplift resistance. The uplift resistance tended to change substantially in linear proportion with the wing diameter ratio at all the pile-end depths. From the results of Figs. 3 and 4, the

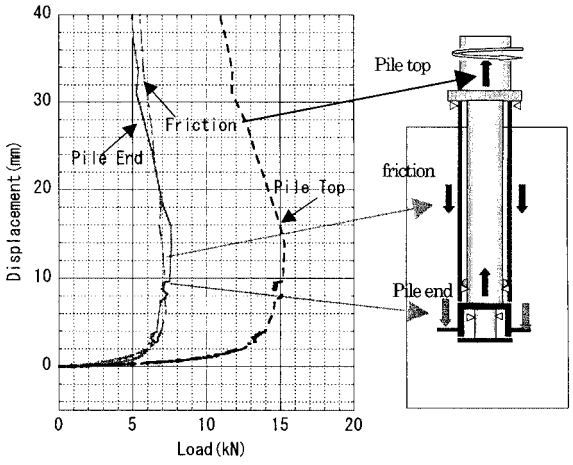

Fig. 2 Relationship between uplifting load and displacement

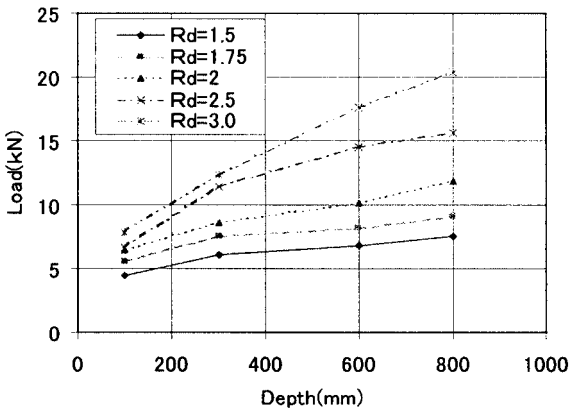

Fig. 3 Relationships between depth and uplift resistance

authors presume that the shear fracture zone has a roughly cylindrical shape, and the height of the cylinder converges upon a certain value when the pile-end depth is large.

Fig. 5 shows the relationship between wing stress, which is the quotient of the pile-end resistance divided by the wing area, and the wing diameter ratio (Rd). The wing stress increased as the wing diameter ratio decreased, indicating that the anchoring effect increased with decreasing wing diameter ratio. On the other hand, **Fig. 6** plots the relationship between pile-end uplifting resistance and the pile diameter of specimens having the same wing diameter (Dw = 100 mm). The graph also shows that the pile-end uplifting resistance increases with decreasing wing diameter ratio. It is inferred from the results that the diameter of the cylindrical soil fracture zone does not increase upward, but rather, it decreases to converge upon some value between the wing diameter and the pile diameter.

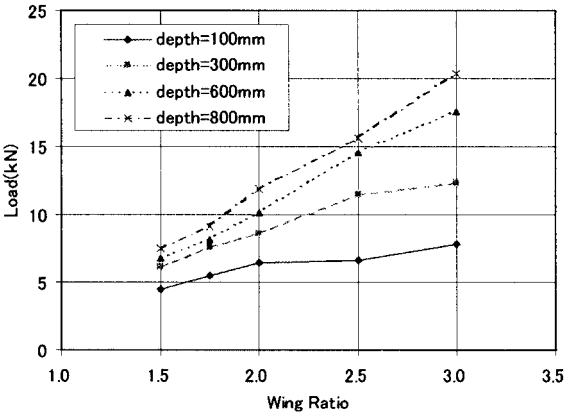

Fig. 4 Relationships between Rd and uplift resistance

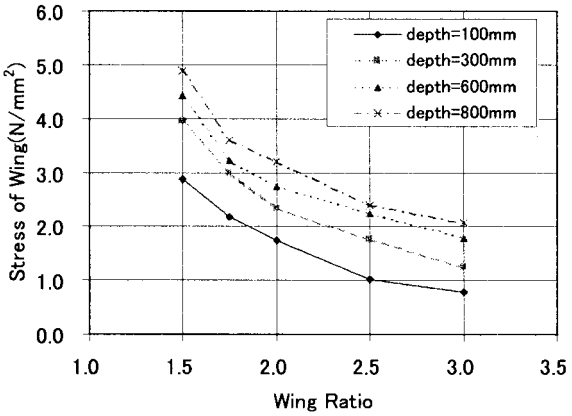

Fig. 5 Relationships between Rd and stress of wing

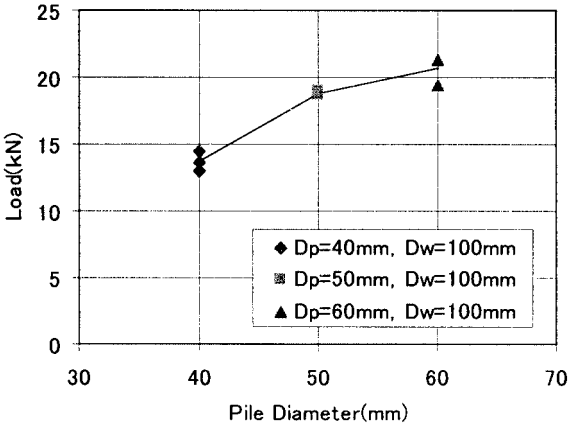

Fig. 6 Relationships between Dp and uplift resistance

4. Verification of Shear Fracture Zone by Visible Tests

4.1 Test equipment

For actually seeing the state of soil, the authors carried out visible tests (sectional soil observation) using a soil tank shown in **Fig. 7**. It is a cylindrical tank 1,000 mm in diameter and 1,000 mm in height, and is equipped with a water supply and drain system at the bottom. The tank wall is divided into horizontal cylindrical segments 50 mm in height (some are 25 mm in height) so that sand layers are easily formed one on another in filling the tank with model soil. The tank wall is divisible also vertically into two semicylinders so that the influence of pile driving and uplifting on the soil can be observed at a section by dividing it into two halves. The model soil was formed by dropping sand from above, and its relative density was controlled to about 80%.

4.2 Test procedures

The specimen piles had a pile diameter (Dp) of 40 mm and a wing diameter ratio of 2 (Dw = 80 mm), and the tests were carried out on the following three cases: (1) pile driving by rotation only, (2) burying (forming the model soil after setting a specimen pile at a prescribed position) and uplifting, and (3) driving by rotation and uplifting. With respect to the pile confining pressure of the soil, two cases were tested: one in which no confining pressure was applied and the other in which only an axial pressure of 300 kPa was applied.

The model soil was formed using dry sand, and colored sand was laid between sand layers each 50 or 25 mm thick to facilitate the observation of sand movement. Water was introduced to the tank after the pile driving or uplifting according to cases (1) to (3), drained after it permeated all over the model soil, and then the soil was divided into two semicylinders to observe the sand movement at the section surface. **Photo 1** shows a vertical section of the model soil for observation.

4.3 Results of visible tests

Photos 2 to 5 show some examples of the test results. Whereas it was possible to uplift a pile up to a pile-end displacement of 1 Dw

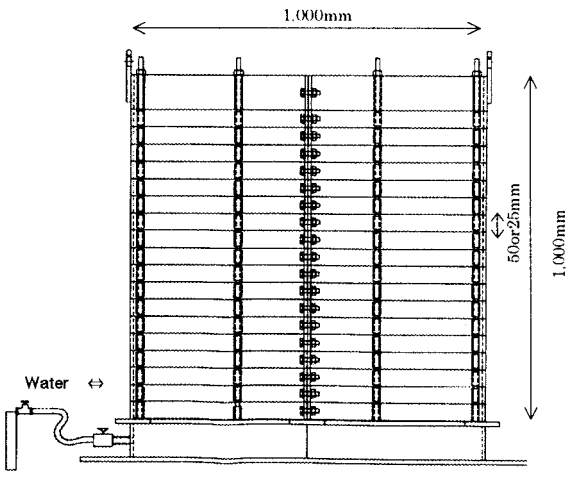

Fig. 7 Visible test tank

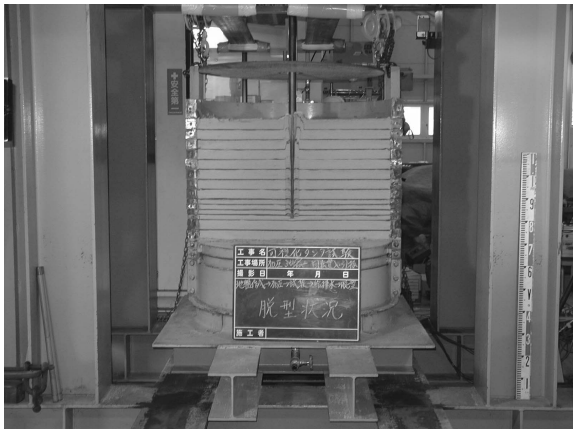

Photo 1 Visible condition

when no confining pressure was applied (Photos 2 and 3), when the axial pressure of 300 kPa was applied (Photos 4 and 5), the resistance at the pile end was so large that the maximum uplifting capacity of the test equipment could produce a pile-end displacement of only 0.1 Dw or so, and it was impossible to confirm a maximum pile-end uplift resistance. Photographs showed the color change of sand in the portion just above the upper surface of the wing (see Photo 3); this resulted presumably from the formation of a compressed region serving as an active wedge when uplifting force was applied. The inversed parabolic shape of the compressed region indicates that, the nearer to the root of the wing, the greater the compression force becomes. No parabolic soil movement was observed in the fracture zone of the soil above the wing, and the shape of the fracture zone

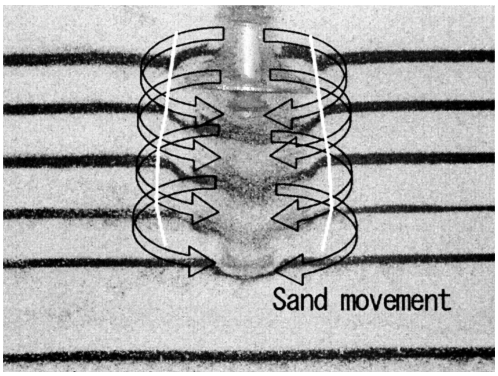

Photo 2 Screw-piling + uplifting test (no confining pressure)

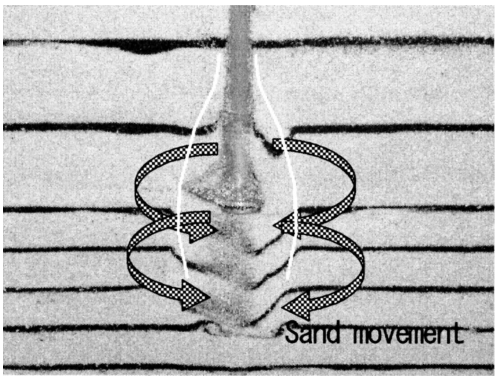

Photo 3 Burying + uplifting test (no confining pressure)

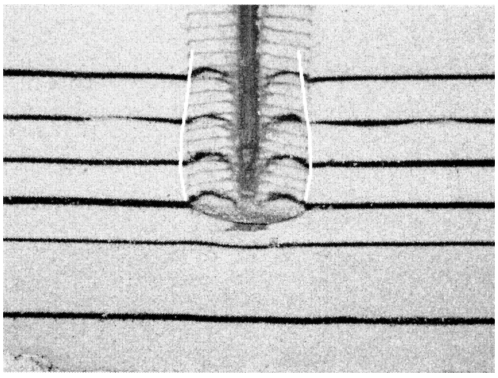

Photo 4 Screw-piling + uplifting test (under confining pressure)

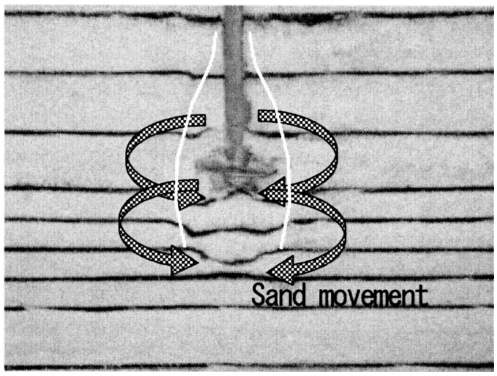

Photo 5 Burying + uplifting test (under confining pressure)

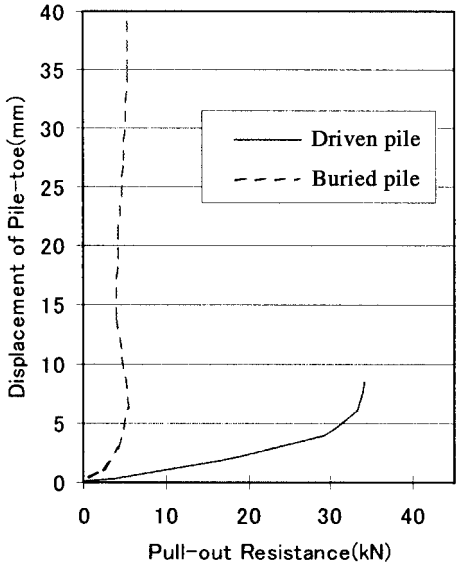

Fig. 8 Uplift resistance

looked to be roughly cylindrical (as contoured with white lines), as expected.

Fig. 8 compares a buried pile and a spirally driven pile in terms of uplift resistance. The uplift resistance of a driven pile was roughly 5 times that of a buried one, which seems to indicate that the soil around the pile was compacted by the driving force of the spiral wing. Photo 4 shows that the sand has moved upward by a distance roughly corresponding to the pile displacement per rotation during

the passage of the wing. This indicates that the wing exerts pile-driving force by pressing on the soil above the upper surface, leaving only a small soil disturbance after the pile-driving work.

5. Earth Pressure Measurement

5.1 Measurement method and cases examined

For the purpose of quantifying the influence of the soil lifting resulting from the pile-driving force of the wing on the soil above it observed in the visible tests and confirming the distribution and magnitude of the earth pressure on the shear fracture zone under uplifting loads, the earth pressure during pile driving and uplifting was measured by the authors.

The measurement was done using the same model-soil tank for the uplifting tests equipped with pressurizing facilities and installing earth pressure gauges 30 mm in diameter at positions about 20 mm from the wing edge to measure horizontal earth pressure (see the right-hand side of **Fig. 9**). The confining pressures of the soil were set as follows: the axial pressure at 300 kPa and the lateral pressure at 150 kPa.

The measurement was done on the following cases: (1) the pile diameter (Dp) was kept constant at 40 mm and the wing diameter ratio (Rd) was changed to 1.5, 1.75, 2.0, 2.5 and 3.0; and (2) the wing diameter (Dw) was kept constant at 100 mm and the pile diameter (Dp) was changed to 40, 50 and 60 mm.

5.2 Measurement results

Fig. 9 shows the earth pressure readings as a pile was driven by rotation and its end passed the depths plotted along the ordinate. The reading of an earth pressure gauge fell once while a pile end approached the position of the gauge from above, then as the pile was driven deeper the reading gradually increased, hit a maximum value nearly equal to that of a passive earth pressure as the wing passed the position of the gauge and went further down, and finally decreased gradually again. The initial fall of the earth pressure resulted presumably from the decrease in the pressure of the soil above the position owing to the driving force of the wing. At the uplifting tests, whereas the earth pressure on the wing lower surface fell rapidly with the displacement under the tensile load, that on the upper surface showed a tendency to increase. In the displacement range where the axial load was the largest, earth pressure changed in all the cases as shown in **Figs. 10 and 11**, forming a trapezoidal curve: it increased to nearly equal to the passive earth pressure near the wing, and it decreased to a value nearly equal to the earth pressure at rest at about 2 Dw above the wing.

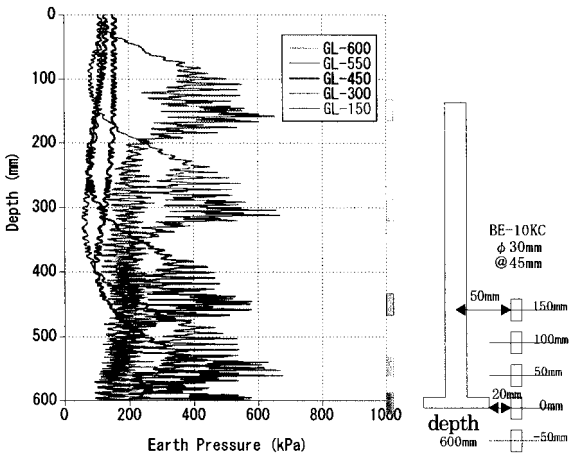

Fig. 9 Earth pressure during pile driving

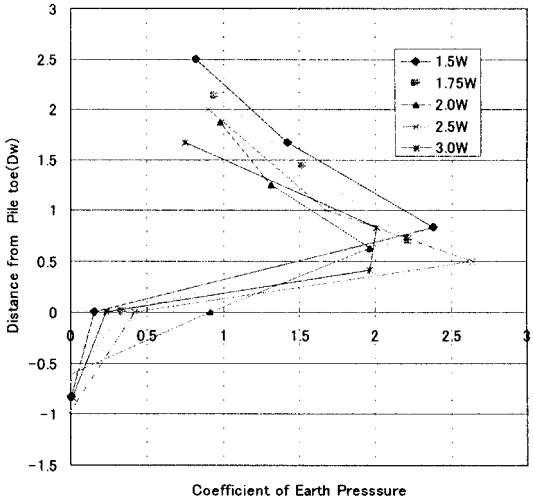

Fig. 10 Distribution of earth pressure (Dp: constant)

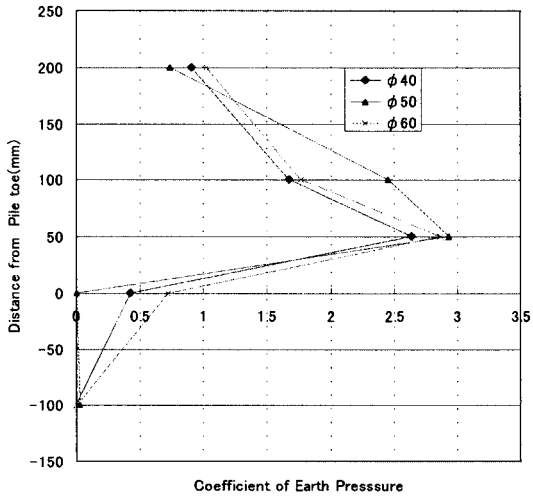

Fig. 11 Distribution of earth pressure (Dw: constant)

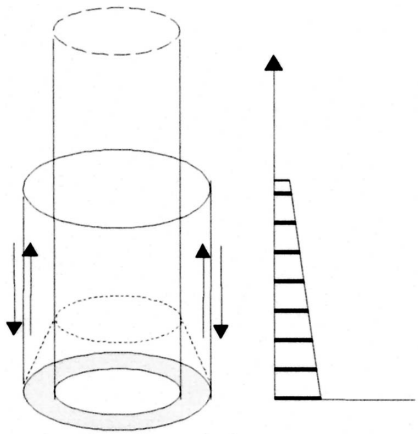

Fig. 12 Uplift resistance mechanism

The above results indicate that the pile-end resistance of a winged pile results from a shear fracture zone and earth pressure distributed in the shape of a truncated cone acting on the fracture zone, as schematically shown in **Fig. 12**.

6. Closing

Through uplifting tests, visible tests and earth pressure measurement using model screwed piles, the characteristics of the uplift resistance of screwed piles were studied, and the shape of the shear fracture zone formed by the pile driving was estimated. As a result, it became possible to estimate the shape of the shear fracture zone and the magnitude and range of the confining pressure of soil acting on the fracture zone. The authors intend to apply these results to the uplifting test results of real-size screwed piles and the estimation and formulation of uplift resistance of screwed piles.

References

1) Saeki, E., Hirata, H., Ohsugi, F.: Results of Uplift Test of Screwed Steel Pile with Wing. Proceedings of the 35th Japan National Conference on Geotechnical Engineering, Jun. 2000, p. 1803-1804
2) Nagata, M., Wada, M., Harada H., Miyamoto, K.: Drawing-out Test on a Steel Pile with Linear Strain - Part 2 Result of Test. Summary of Technical Papers of Annual Meeting, Architectural Institute of Japan (Hokuriku Branch). Aug. 2002, p. 513-514
3) Saeki, E., Nagata, M., Hirata, H., Wada, M.: Model Test System of Screwed Steel Pile. in Proceedings of the 36th Japan National Conference on Geotechnical Engineering. July. 2001, p. 1623-1624